PS Seismic Expression of Karst-Related Features in the Persian Gulf and Implications for Characterization of Carbonate Reservoirs*

Caroline M. Burberry[1], Shelby R. Chandler[1], and Christopher A-L. Jackson[2]

Search and Discovery Article #30411 (2015)**
Posted August 17, 2015

*Adapted from poster presentation given at AAPG 2015 Annual Convention and Exhibition, Denver, Colorado, May 31 – June 3, 2015

[1]Department of Earth and Atmospheric Sciences, University of Nebraska-Lincoln, Lincoln, Nebraska, USA (cburberry2@unl.edu)
[2]Department of Earth Science and Engineering, Imperial College London, London, United Kingdom

Abstract

Karstification can have a positive and negative effect on carbonate reservoirs. For example, dissolution during karstification can enhance inter- and intra-granular porosity and permeability, whereas cave collapse can generate mega-pores and completely alter reservoir geometry and continuity. Karst may also pose challenges to drilling due to the unpredictable and highly variable porosity and permeability structure of the rock, and corresponding difficulty in predicting drilling mud-weight. Some of the largest karst-related features are imaged by seismic reflection data, thus they can be mapped directly, improving carbonate reservoir characterization and allowing development of safer drilling programs. In this study we use time-migrated 2D seismic reflection data to determine the distribution, scale and genesis of karst in a 3 km thick, Jurassic-Miocene carbonate-dominated succession in the Persian Gulf. We map 34 near-circular karst features on the top-Turonian regional unconformity that marks the top of the Upper Cretaceous Sarvak Formation. These sinkhole-like features are 0.8–10.2 km in diameter and 15–80 m deep, and are onlapped by overlying Coniacian strata, thus constraining their age. Additional subsidence, driven by differential compaction above in the stratigraphic succession overlying the sinkholes, occurred until the Early Miocene. We interpret that a 1100 m thick poorly imaged interval developed immediately below the sinkholes is related to subterranean collapse or poor seismic imaging below the highly geologically and geophysically heterogeneous karstified surface. There is no relationship between sinkhole diameter and depth, suggesting that the sinkholes did not widen as they deepened. Instead, the distribution of sinkholes along pan-African fault trends or around salt domes suggest a formation mechanism of cave collapse associated with fluid movement along pre-existing fault or fracture networks. These data indicate that seismic-scale karst features may be deep, wide and areally widespread at specific stratigraphic levels, suggesting that sub-seismic-scale karstic features may be even more widespread. Our study indicates that seismic reflection data can and should be used to determine the extent and scale of karstification with the specific aim of improving the characterization of carbonate reservoirs.

SEISMIC EXPRESION OF KARST-RELATED FEATURES IN THE PERSIAN GULF AND IMPLICATIONS FOR THE CHARACTERIZATION OF CARBONATE RESERVOIRS

Caroline M. Burberry[1], Shelby R. Chandler[1], & Christopher A-L. Jackson[2]

[1]University of Nebraska-Lincoln, [2]Imperial College London

cburberry2@unl.edu

eas2.unl.edu/~cburberry/

basinsresearchgroup.com

1. Introduction

- Karstification positively and negatively impacts the quality of carbonate reservoirs.
- Dissolution can enhance inter- and intra-granular porosity and permeability
- Cave collapse can generate mega-pores (Figure 1)
- Characterizing heterogeneity should consider the possibility of multiple zones of enhanced poroperm
- Also consider potential for connectivity by sub-vertical pipes of enhanced dissolution
- Karstified regions may be challenging to drill - unpredictable & variable poroperm, difficulty in predicting drilling mud-weight
- Some of the largest karst-related features are imaged in seismic reflection data, thus can be directly mapped, improving carbonate reservoir characterization & allowing development of safer drilling programs.

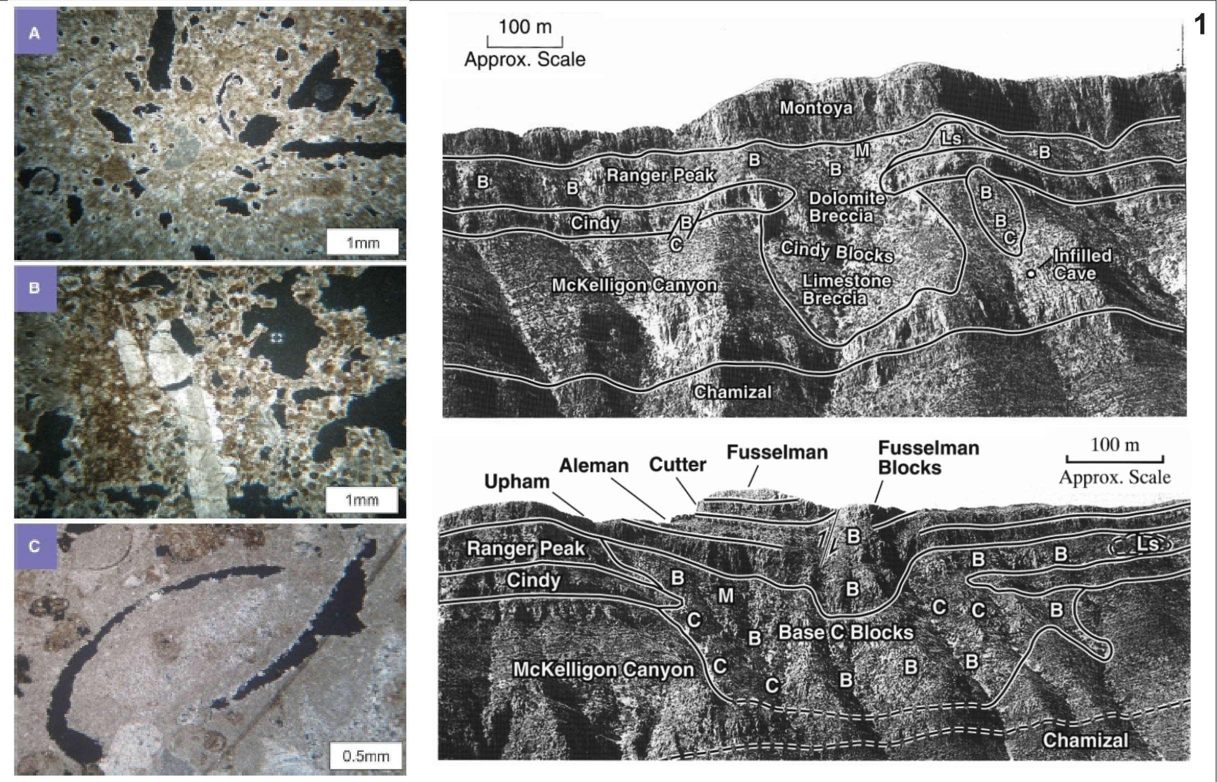

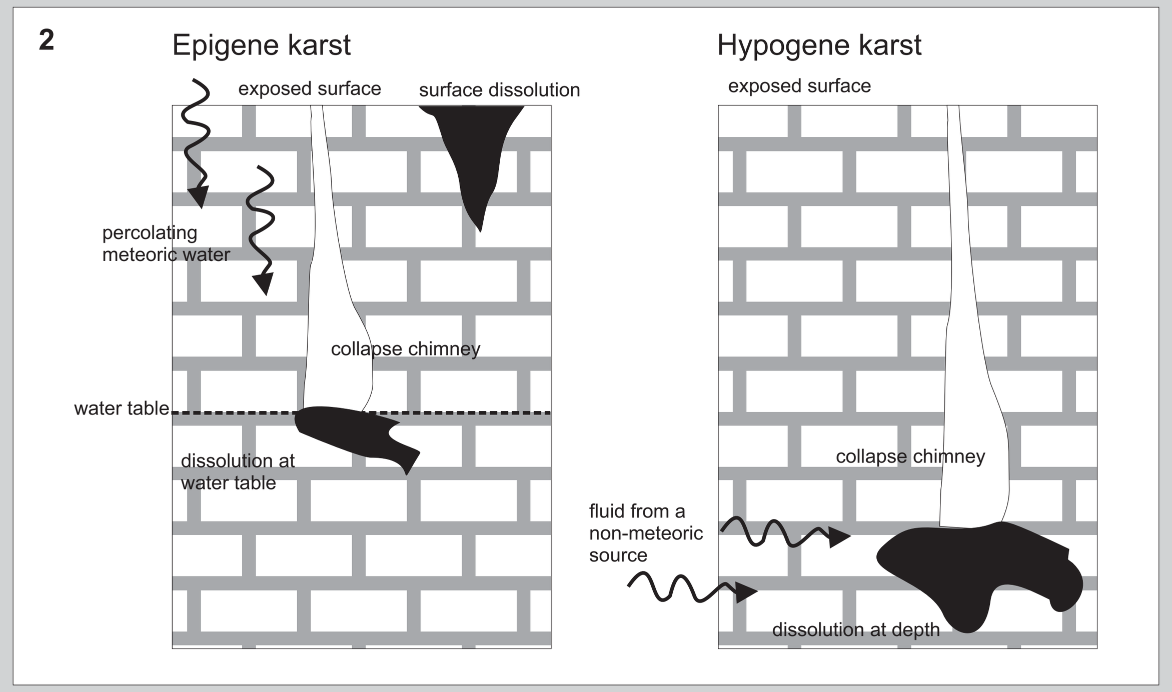

Figure 1 (left): Variable scales of karstification. (a-c) mm-scale porosity generated by dissolution, from Mehrabi & Rahimpour-Bonab (2014), (d,e) caverns filled with collapse breccia from the Franklin Mts, TX, from Lucia (1995).

Figure 2 (above, left): Schematic illustrating the variable fluid sources and potential structures formed under epigene and hypogene karst conditions

- Karst features can develop either by hypogene or epigene processes (Figure 2).
- Epigene karstification, dissolving fluid is meteoric
- Produces depressions and fissures in the exposed surface, which widen upward and show a positive linear relationship between width and depth on the paleo-exposure surface.
- Also dissolution at the water table, forming collapse-related structures, which widen and deepen downward.
- Hypogene karstification, dissolving fluid is not meteoric in origin
- Fluid enters the system and is recharged from below
- Dissolution of material occurs at depth, with eventual cavern collapse forming collapse structures

2. Methods

In this study we use time-migrated 2D seismic reflection data to determine the distribution, scale and genesis of karst in a 3 km thick, Jurassic-Miocene carbonate-dominated succession in the Persian Gulf (Figures 3-5). Reflection events were tied to well data from two nearby wells, IMD-1 and IE-1 (Figure 6; Swift et al., 1998).

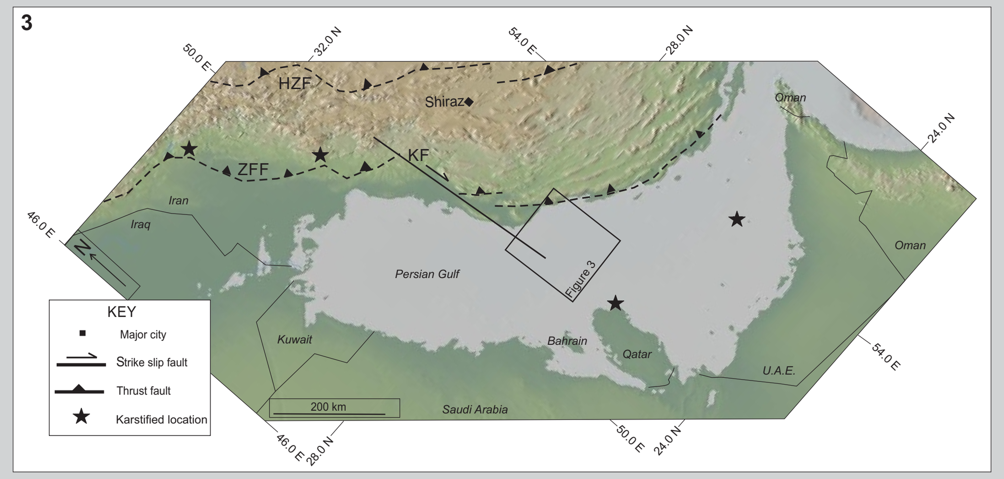

Figure 3 (above): Map locating the study area within the Persian Gulf, on a DEM derived from GeoMapApp. ZFF; Zagros Frontal Fault and HZF; High Zagros Fault. KF: Kazerun Fault, a key basement fault in the region. Black stars mark other karsted locations in the region.

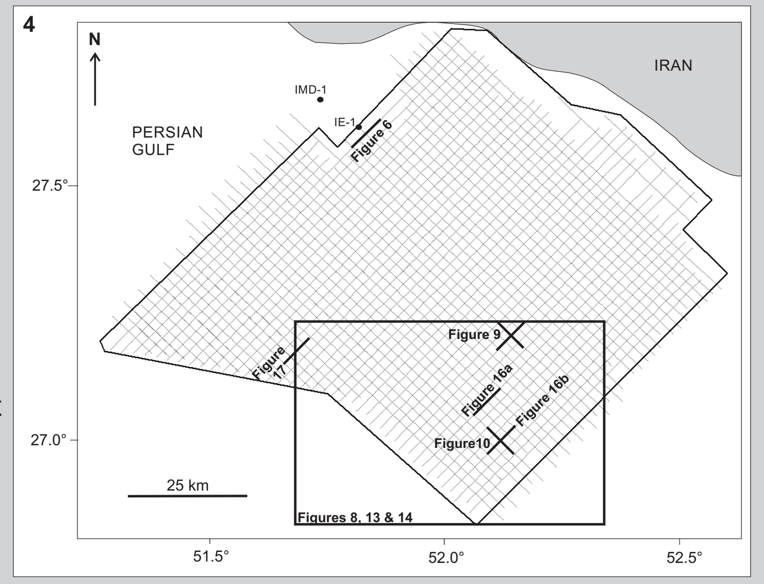

Figure 4 (above): Map showing the layout of the seismic grid in this dataset, as well as the location of the wells used for correlation and horizon identification. Bounding boxes and lines show locations of data presented in other figures.

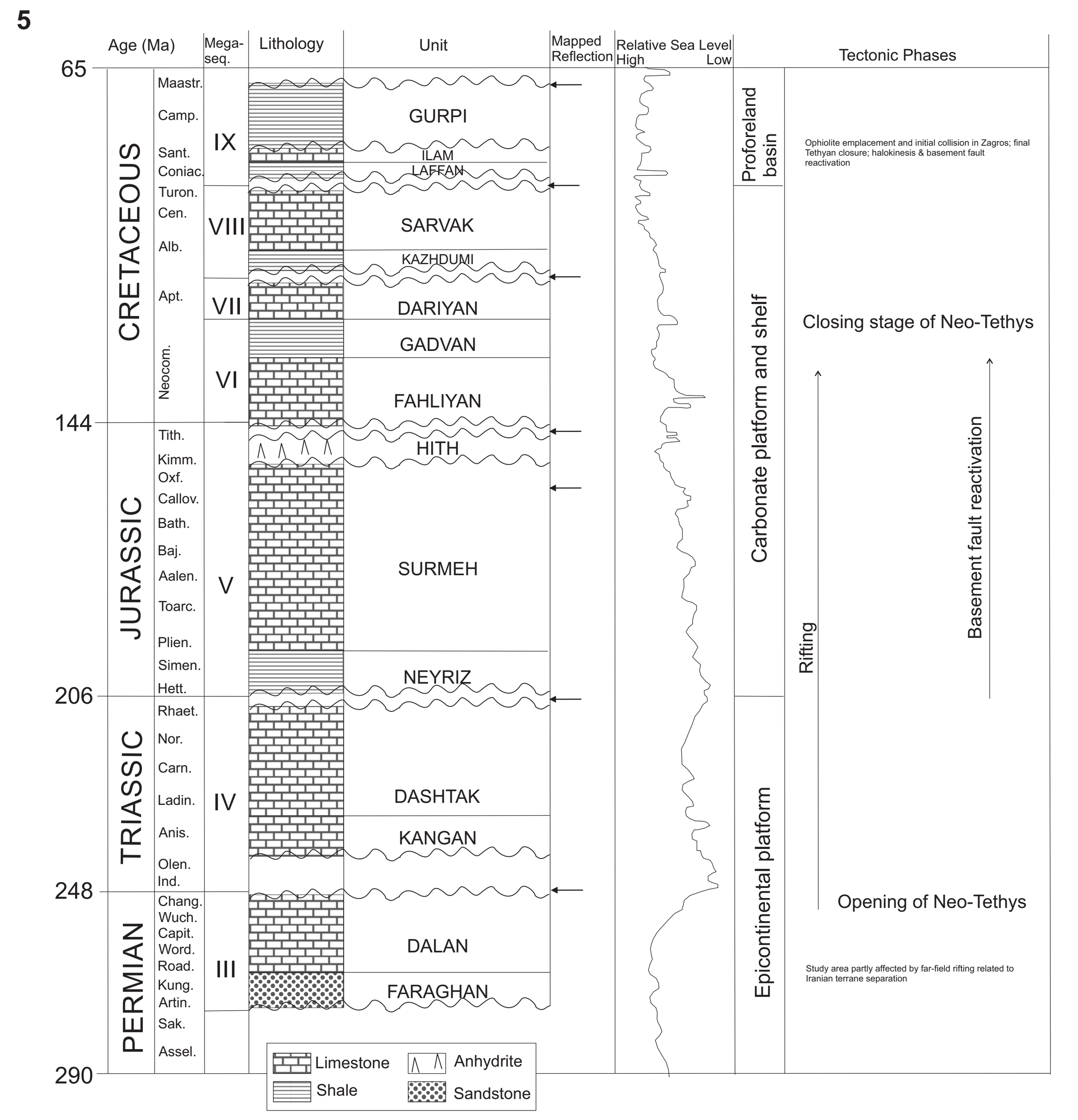

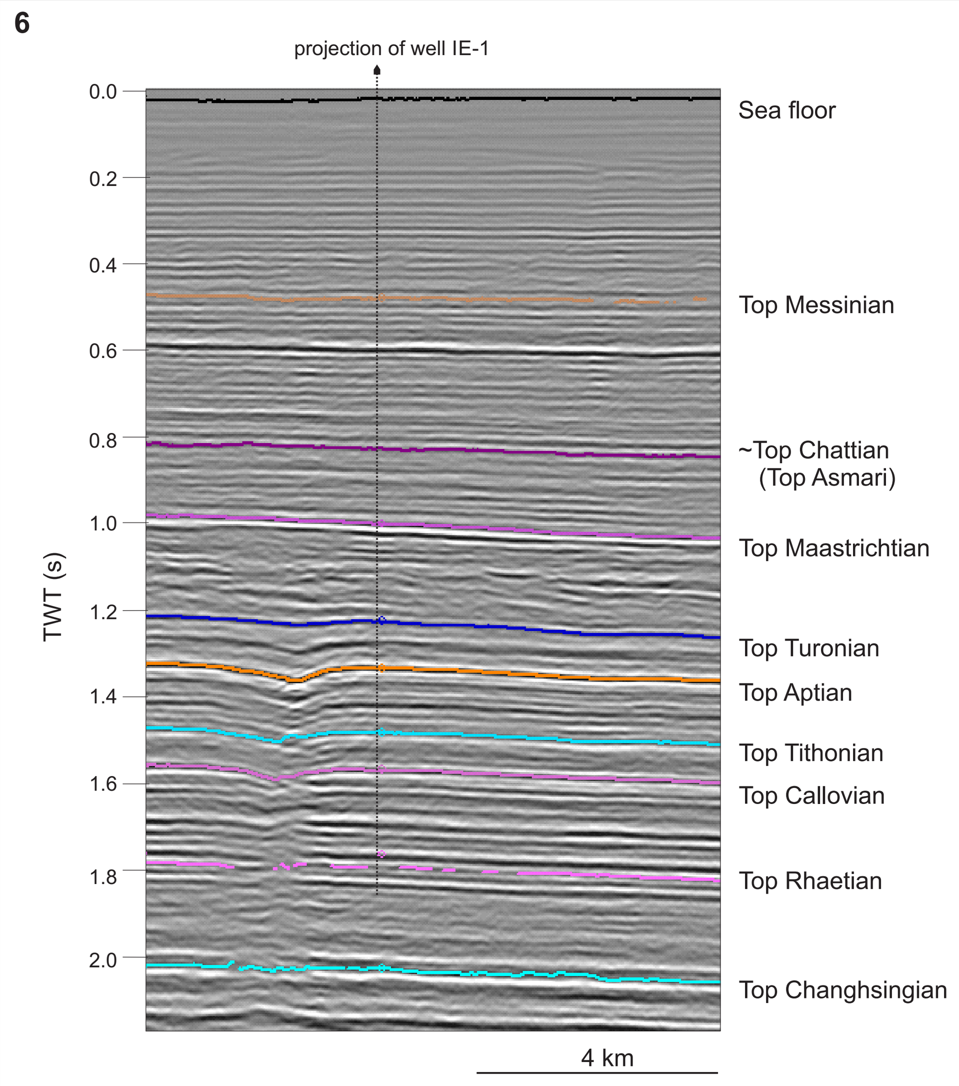

	Formation Tops in TWT (s)		Projected marker depths from this dataset in TWT (s)
	IMD-1	IE-1	
Top Messinian	0.43	-	0.47
~Top Chattian (Top Asmari)	0.72	0.83	0.82
Top Maastrichtian	1.09	1.06	0.99
Top Turonian	1.2	1.11	1.21
Top Aptian	1.31	1.34	1.31
Top Tithonian	1.47	1.52	1.46
Top Callovian	1.69	1.6	1.58
Top Rhaetian	1.84	1.67	1.76
Top Changhsingian	1.9	-	2.2

Figure 5 (left): Tectonostratigraphic column showing the units of interest in the Permian – Cretaceous section, together with important regional tectonic events and a global sea level curve. The global sea level curve and megasequence information are from Alavi (2004). Arrows mark the reflection events mapped in the study.

Figure 6 (above): Well-tie from wells given in Swift et al. (1998) to the closest seismic line and the depths in TWT of each mapped reflection on this line. Mapped reflections are arrowed on Figure 5 and the location of the seismic segment is shown on Figure 4.

3. Results

OVERALL STRUCTURE >>>

- NW-SE-striking normal faults and two prominent domes (Figure 7a) on top Rhaetian reflection.
- Faults not observed on and thus die-out below the Turonian Unconformity (Figure 7b).
- Turonian Unconformity dips gently to the NE, with a series of low-amplitude anticlines in the NE of the dataset.

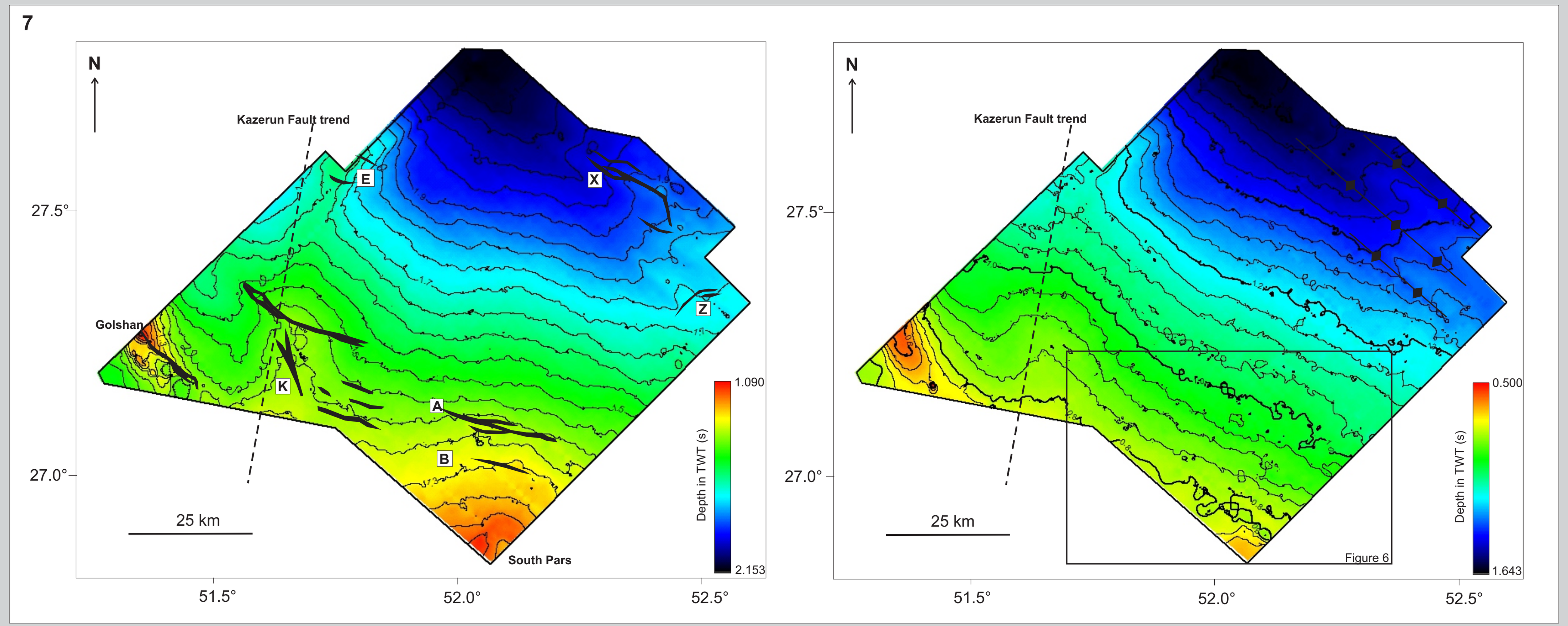

Figure 7: Top structure maps of the Rhaetian and Turonian reflections. Fault cuts and the trend of the Kazerun Fault are shown. Faults and structural highs (the Golshan and South Pars structures) on the top Triassic reflection are labeled after Bordenave (2003).

Figure 8: Detailed contour maps of the top Callovian, top Tithonian, top Aptian and top Turonian reflections. Only the region where the most features are found is shown, so that detail may be seen. Sub-circular depressions can be observed in the contours. The locations of the features shown in Figures 7 and 9 are marked by black boxes.

DETAILED STRUCTURE >>>

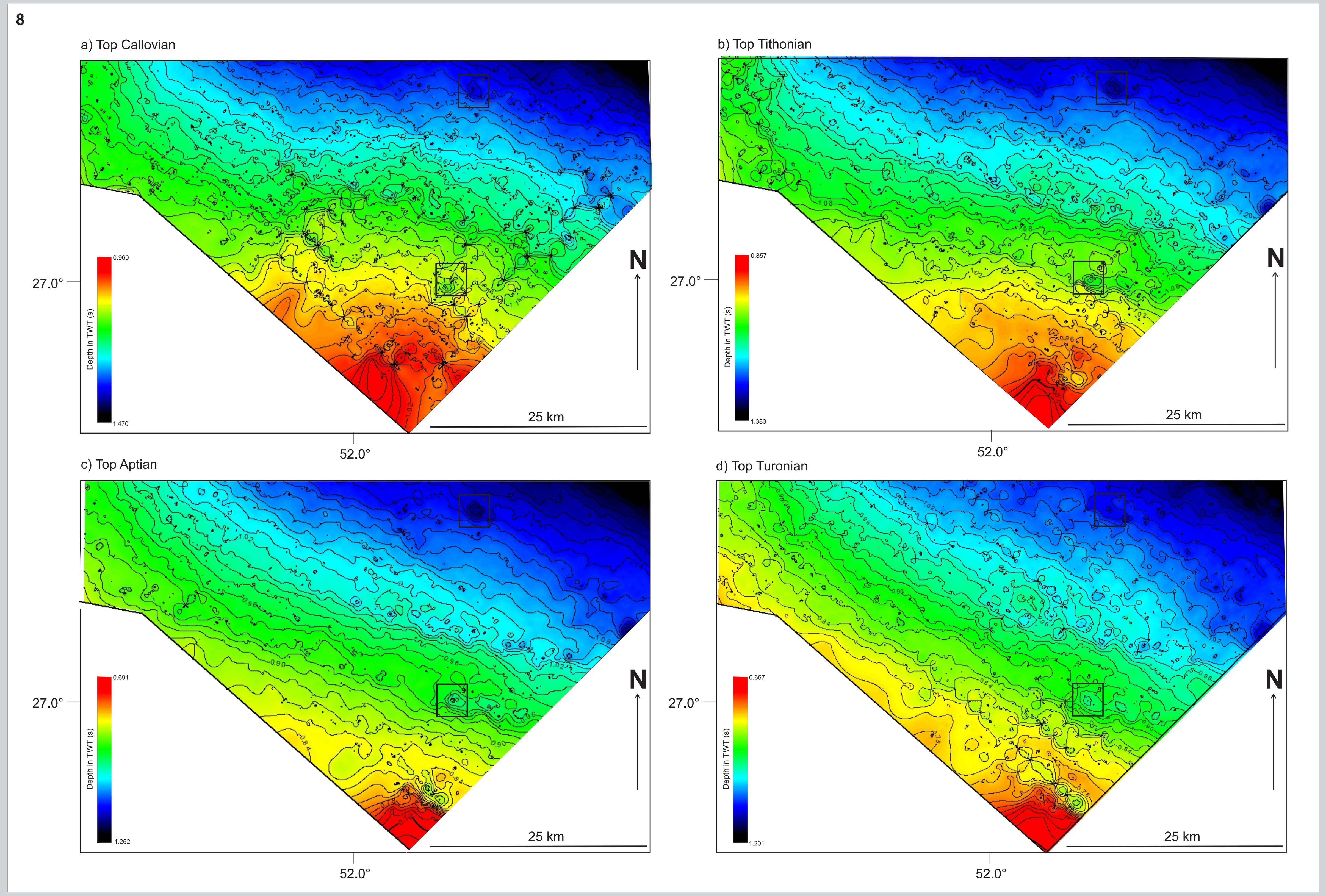

SEISMIC EXPRESION OF KARST-RELATED FEATURES IN THE PERSIAN GULF AND IMPLICATIONS FOR THE CHARACTERIZATION OF CARBONATE RESERVOIRS

Caroline M. Burberry[1], Shelby R. Chandler[1], & Christopher A-L. Jackson[2]

[1]University of Nebraska-Lincoln, [2]Imperial College London

cburberry2@unl.edu

University of Nebraska Lincoln

eas2.unl.edu/~cburberry/

Imperial College London

basinsresearchgroup.com

3. Results Cont'd.

DETAILED STRUCTURE >>>

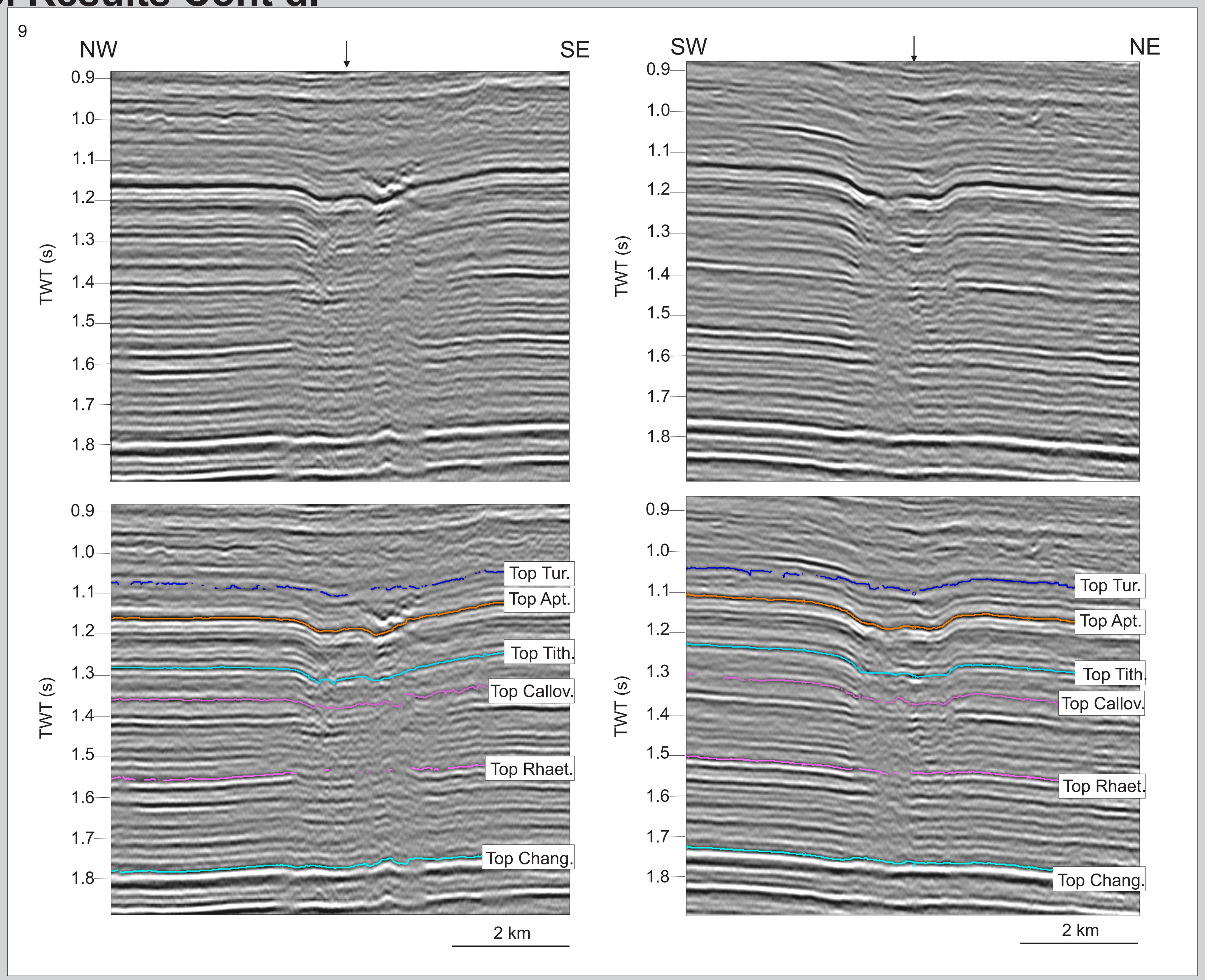

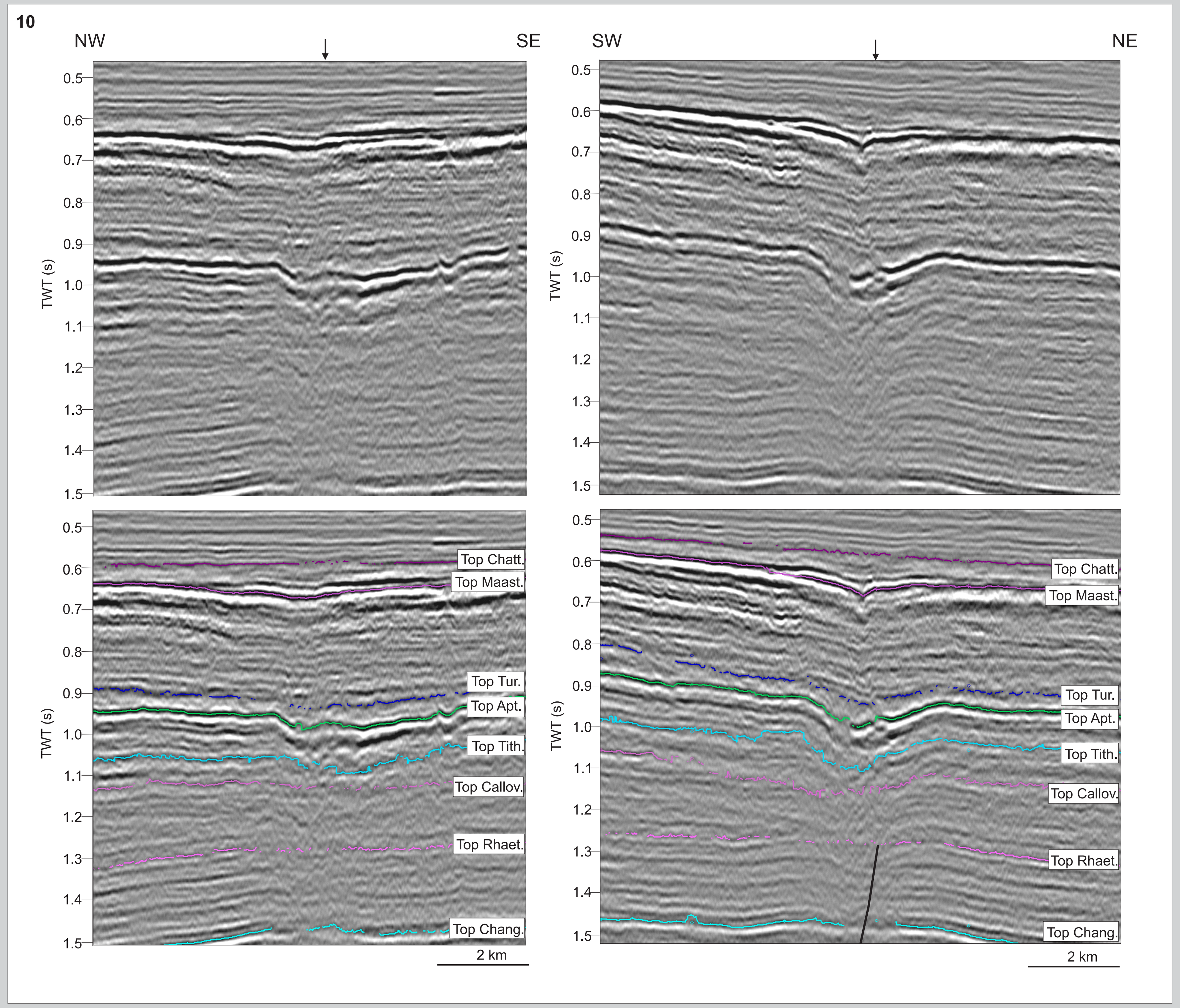

- Using detailed contour maps (Figure 8) and line-by-line inspection of the dataset, we map 43 seismic-scale features
- Features expressed as vertical, sub-circular columns of chaotic reflections capped by downward-deflected depressions that are onlapped by overlying strata, spanning the Jurassic to Upper Cretaceous succession (Figure 9).
- 25% of the features are expressed on the top Maastrichtian reflection, with associated onlapping of overlying clastic units (Figure 10).
- Weak positive correlation between the width and depth of features on each specific horizon (Figure 11), top Aptian features > top Turonian features.
- Top Maastrichtian deflections are typically located vertically above the largest deflection features (Figure 12).

Figure 9: NW and NE-oriented crossing lines showing the morphology of a pipe-like feature forming a vertical zone of chaotic reflections. The arrow marks the point where the lines cross. Both uninterpreted and interpreted lines are shown. The feature deforms horizons from the top Turonian to the top Callovian reflections and significant thinning is noted in the top Tithonian-top Callovian package (the Hith Anhydrite). The location of these seismic segments is marked on Figure 4.

Figure 10 (left): NW and NE-oriented crossing lines showing the morphology of a karst feature forming a vertical zone of chaotic reflections. The arrow marks the point where the lines cross. Both uninterpreted and interpreted lines are shown. The feature deforms horizons from the top Maastrichtian to the top Callovian reflections and significant thinning is noted in the top Jurassic-top Callovian package. The Paleocene-Oligocene package onlaps the deflected top Maastrichtian reflection. The location of these seismic segments is marked on Figure 4.

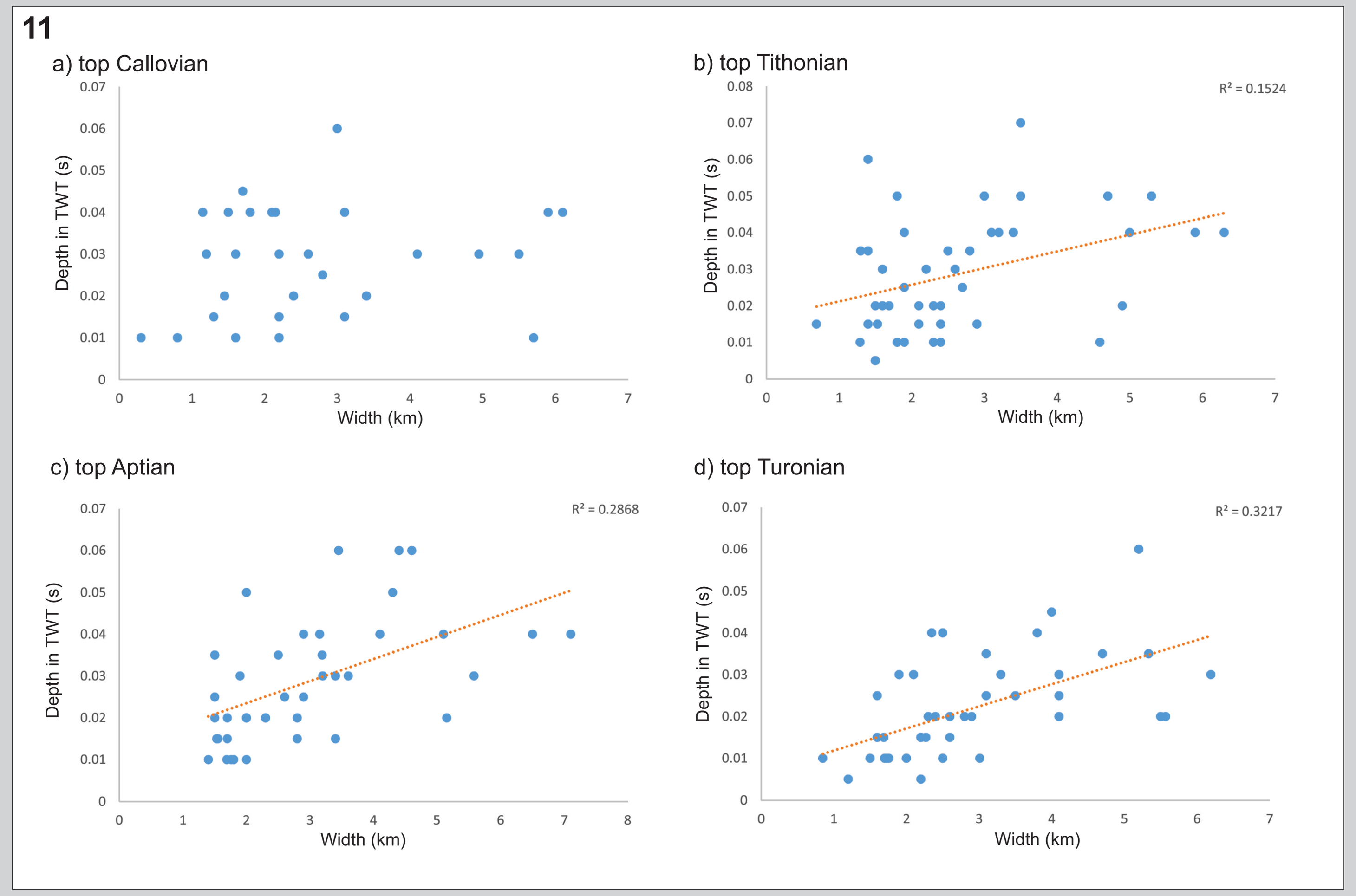

Figure 11 (far left): Graphs showing the variation in depth of the features with changing width, on the top Callovian, top Tithonian, top Aptian and top Turonian reflections. Weak positive correlation between width and depth is noted on the top Tithonian, top Aptian and top Turonian reflections, but not the top Callovian reflection. R^2 values for the best-fit line shown are noted on the graphs.

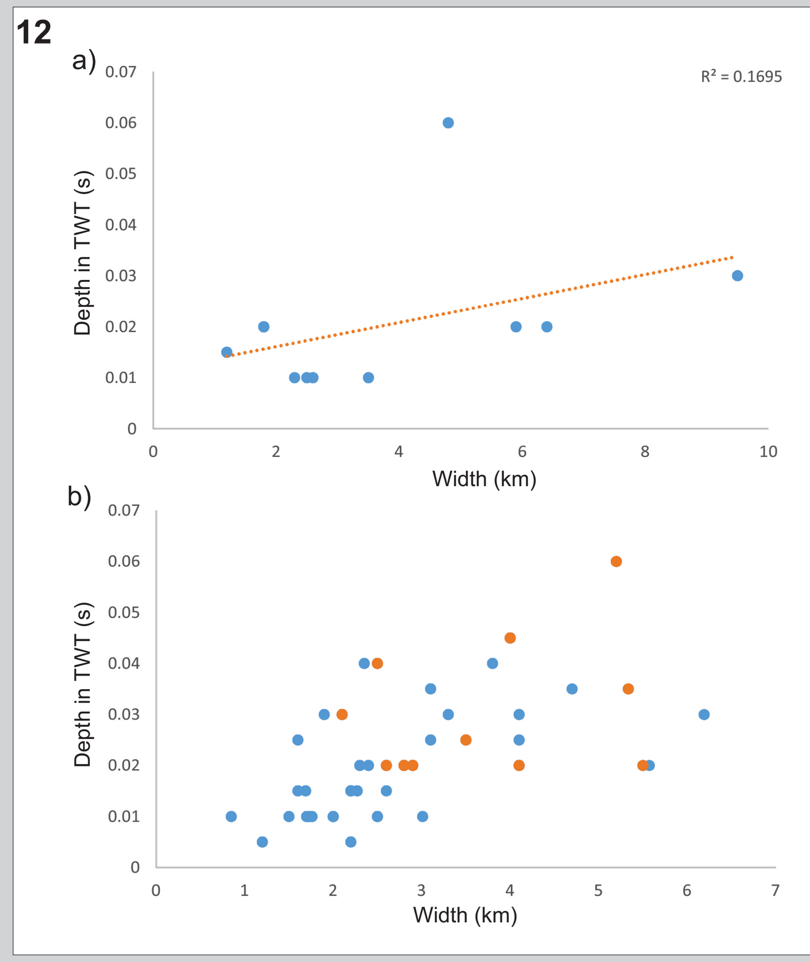

Figure 12 (left): a) Graph showing the variation in depth of the features with changing width, on the top Maastrichtian reflection. Weak correlation between width and depth is noted. The R^2 value for the best-fit line shown are noted on the graph. b) Graph showing width-depth relationship between features on the top Turonian and top Maastrichtian reflections. Blue dots indicate features on the top Turonian reflection with no Maastrichtian counterpart; red dots indicate those Turonian features with associated Maastrichtian deflections. Larger features have associated Maastrichtian depressions.

<<< THICKNESS VARIATIONS

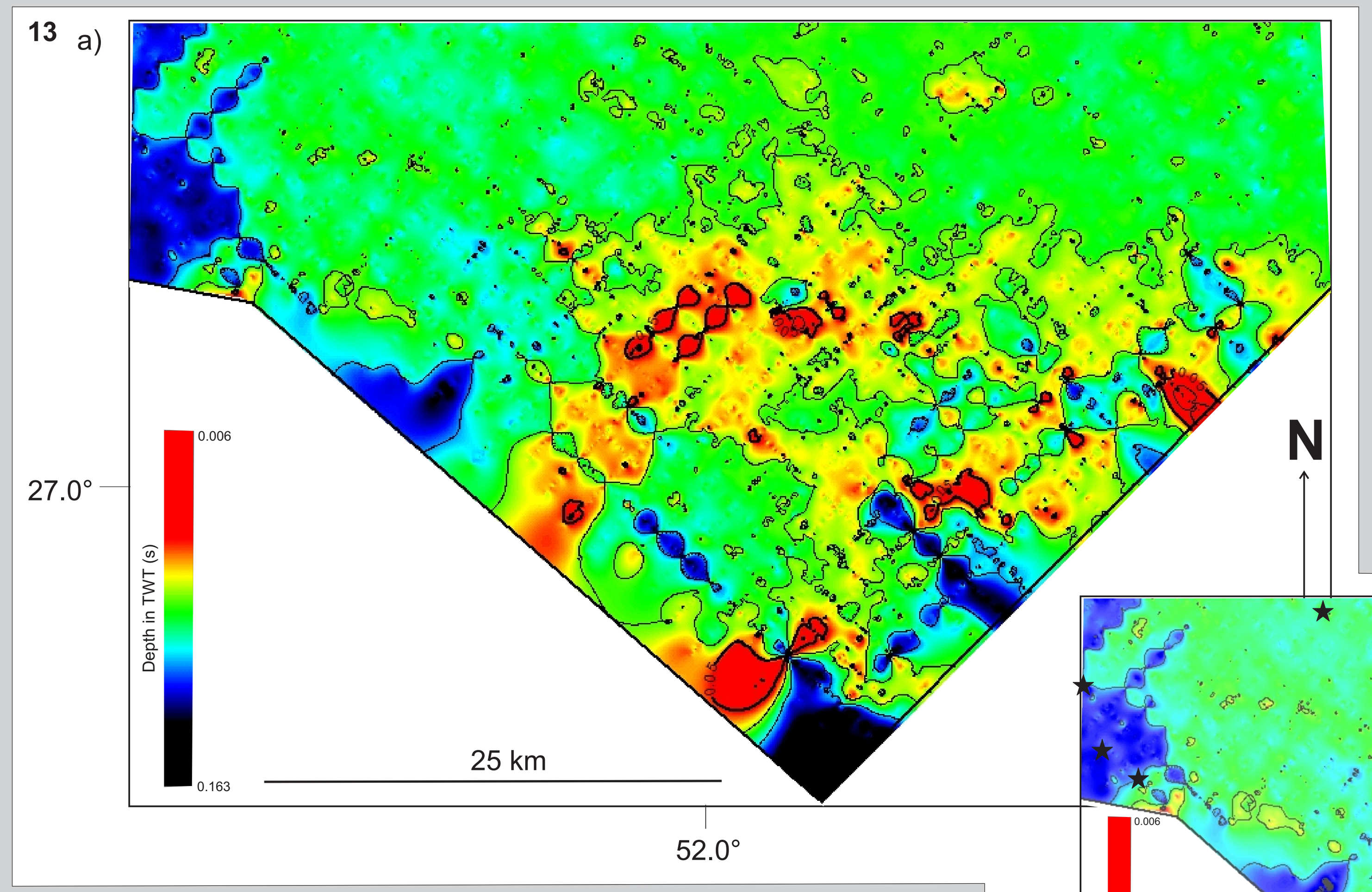

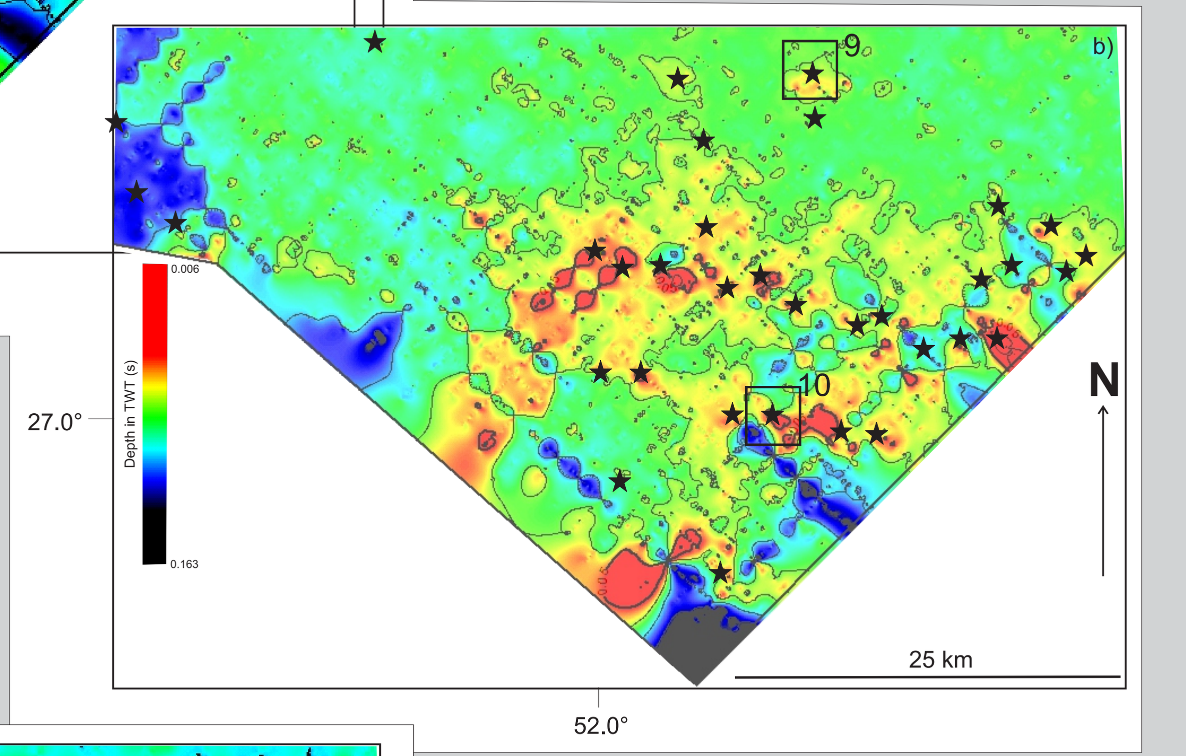

- Thinning of the seismic package between the top Tithonian and top Callovian reflections (Figure 13, see also Figures 9 and 10) observed beneath the features
- Similar thinning observed in the seismic package between the top Callovian and top Rhaetian reflections (Figure 14, see also Figures 9 and 10).

Figure 13 (above, left): Map showing the thickness variation in the top Tithonian-top Callovian seismic package, for the detailed area shown in Figure 8. Overlain black stars in part (b) indicate the locations of mapped pipe-like features, correlating to zones of thinning in this package. The locations of the features shown in Figures 9 and 10 are marked by black boxes.

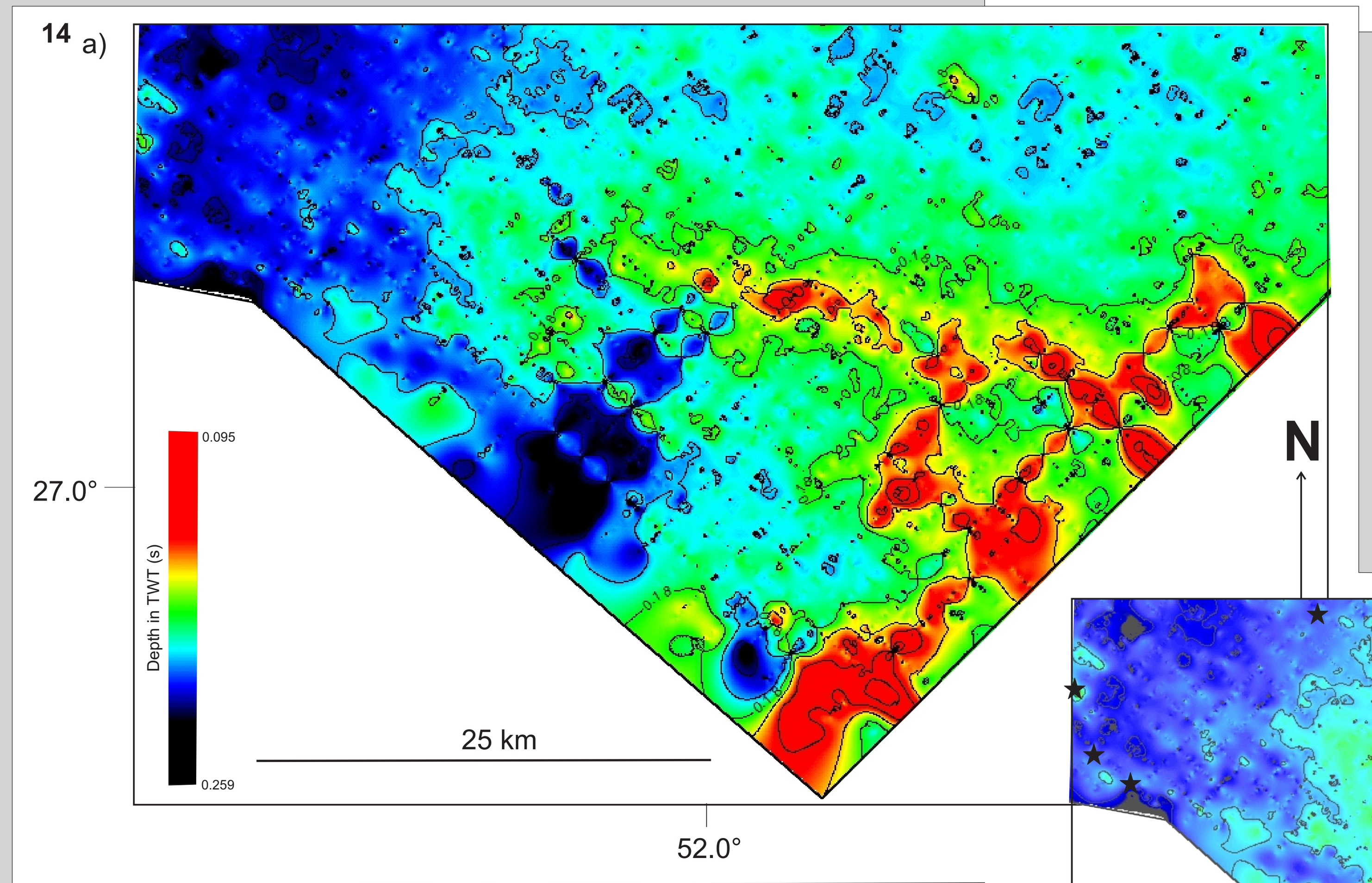

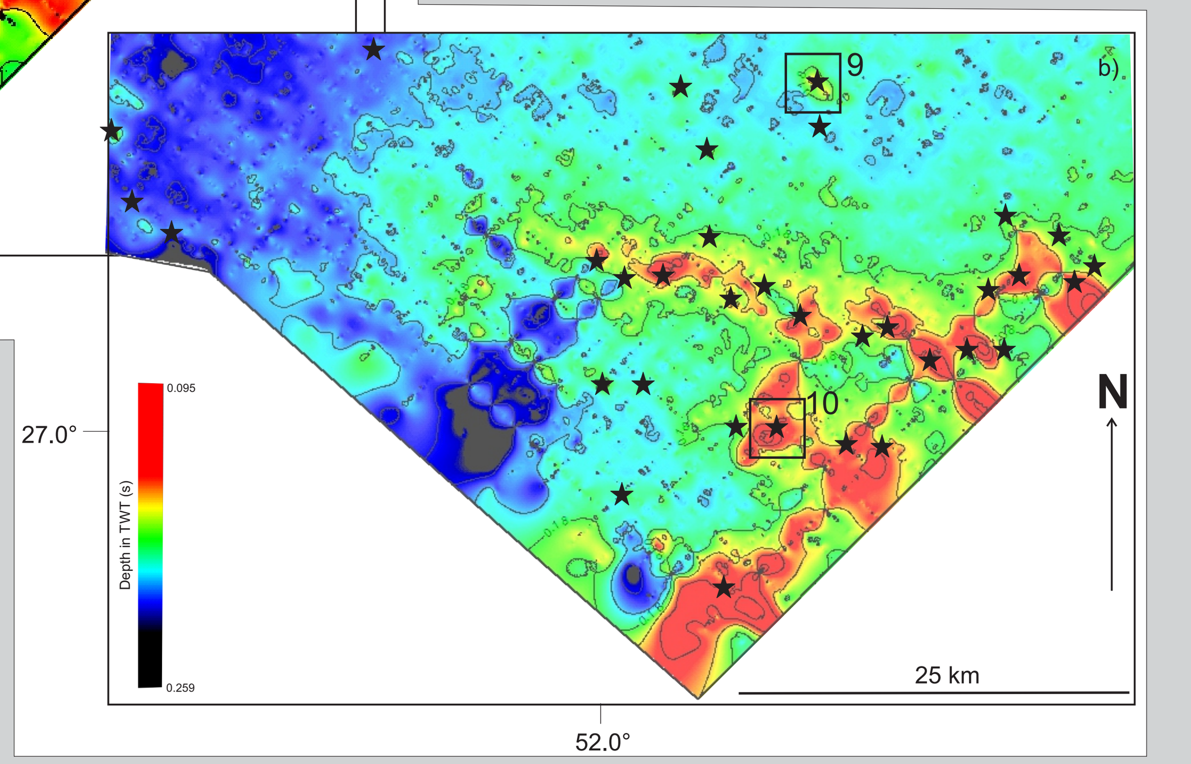

Figure 14 above, right): Map showing the thickness variation in the top Callovian-top Rhaetian seismic package, for the detailed area shown in Figure 8. Overlain black stars in part (b) indicate the locations of mapped pipe-like features, correlating to zones of thinning in this package. The locations of the features shown in Figures 9 and 10 are marked by black boxes.

SEISMIC EXPRESION OF KARST-RELATED FEATURES IN THE PERSIAN GULF AND IMPLICATIONS FOR THE CHARACTERIZATION OF CARBONATE RESERVOIRS

Caroline M. Burberry[1], Shelby R. Chandler[1], & Christopher A-L. Jackson[2]

[1]University of Nebraska-Lincoln, [2]Imperial College London

cburberry2@unl.edu

eas2.unl.edu/~cburberry/

basinsresearchgroup.com

3. Results Cont'd.

FEATURE DISTRIBUTION >>>

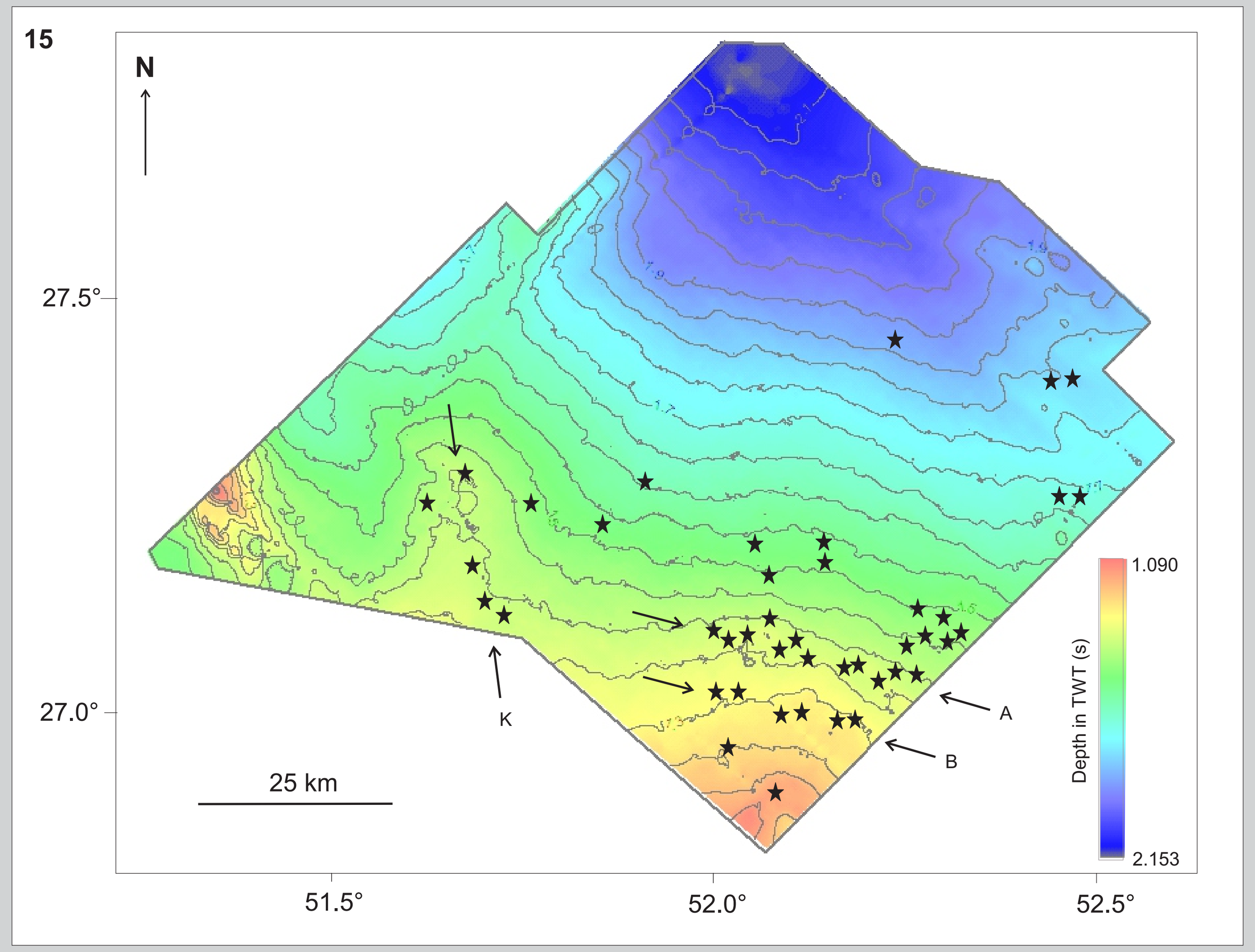

- Features most common in the southern part of the dataset, close to the South Pars Field (Figure 15, see also Figure 7).
- Three subtle linear trends (arrowed on Figure 15), associated with faults A and B (Figure 16) and fault K (Figure 17).

Figure 15: Top structure map of the Top Rhaetian reflection, with associated fault cuts marked in pale grey. Structures discussed in the text are arrowed and labeled. Black stars mark the locations of mapped pipe-like features.

Figure 16: Seismic lines, both uninterpreted and interpreted, showing the relationship of some pipe-like features to fault structures A and B (refer back to Figure 7a for fault morphology). Note that the images shown in part (b) are of the same feature as Figure 10, but this figure is extended to depth to illustrate the fault geometry and associated chaotic reflections.

Figure 17: Seismic line, both uninterpreted and interpreted, showing the relationship of a pipe-like feature to fault structure K (refer back to Figure 7a for fault morphology). Note that in this example the influence of the faulting is more prominent than the influence of dissolution.

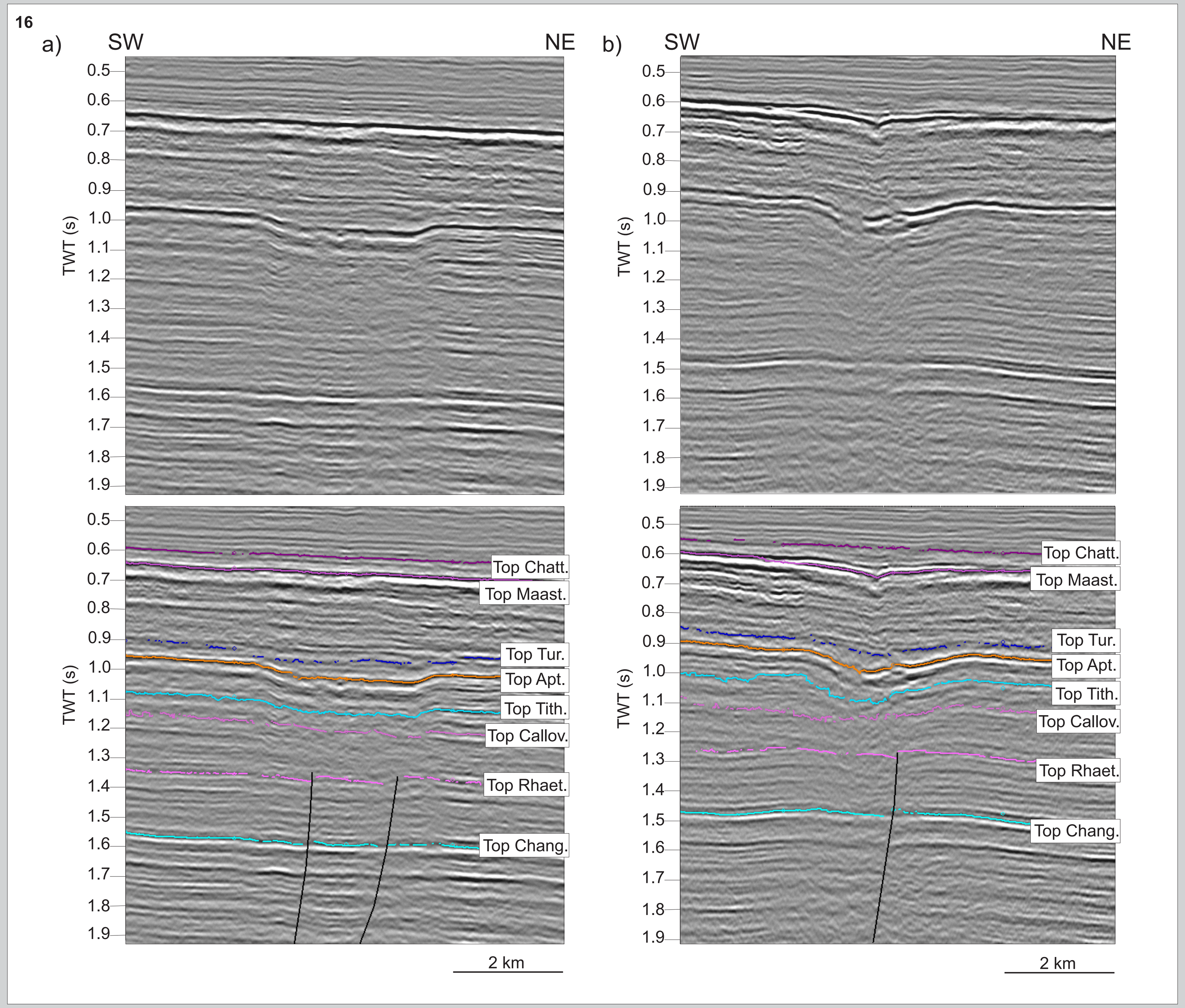

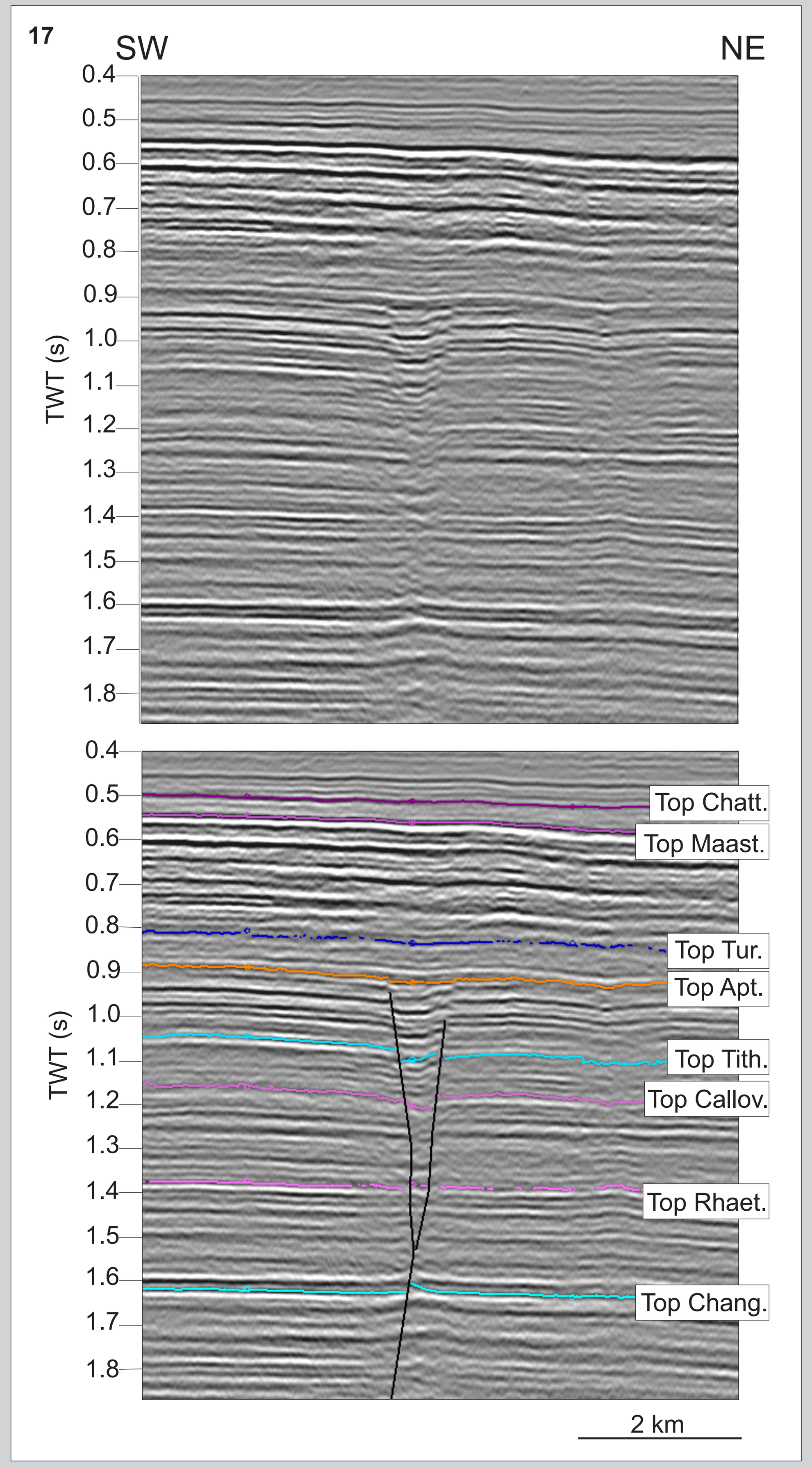

In summary, 43 pipe-like zones of distorted and downward deflected reflection events are observed in the dataset, extending from the top Callovian up to the top Turonian reflection events; occasionally these zones and the associated downward deflection are expressed at the top Maastrichtian reflections, a vertical distance of 1500-2100 m. On the top Turonian and top Aptian reflections there is a weak linear relationship between deflection width and depth, although the features are, on average, wider and deeper on the top Aptian reflection than on the top Turonian reflection, thus they narrow and become shallower upwards. The width-depth relationship is less pronounced on the top Jurassic reflection and is not present for the features at the top Callovian reflection. Marked thinning occurs in the Jurassic section beneath the pipe-like features.

4. Interpretation

- Features are collapse sinkholes, formed by three phases of epigene karstification.
- Phase 1 - generated caverns c. 300m below the contemporaneous free surface that collapsed to form sinkholes in overlying strata as sediment overburden weight increased.
- Phases 2, 3 - Exposure of the paleo-surface at end-Aptian and end-Turonian (Figure 18) increased the width and depth of the sinkholes at these levels.

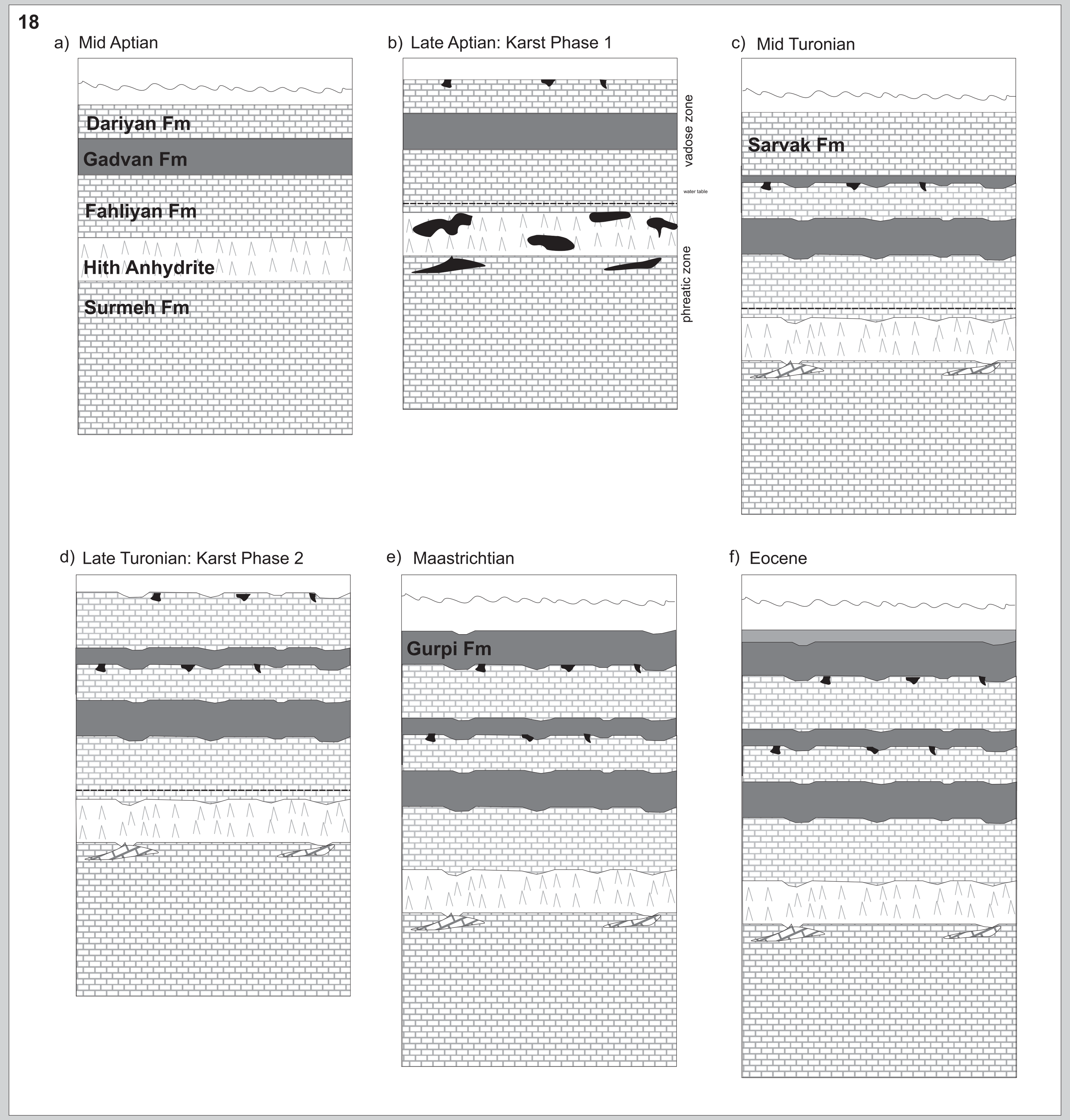

Figure 18: Conceptual diagram showing the development of the seismic-scale karst features in the study area. a) deposition of units up to and including the Aptian Dariyan Formation; b) relative sea level fall and uplift combine to expose the Dariyan Formation in the Late Aptian. Karstification occurs on the exposed surface and dissolution occurs in the Hith Anhydrite and Surmeh Formations, close to the water table, leading to collapse of overlying strata; c) deposition of units up to and including the Sarvak Formation. The increased weight of overburden causes further collapse of caverns within the Hith Anhydrite and Surmeh Formation, deforming the sequence; d) relative sea level fall and uplift combine to expose the Sarvak Formation in the Late Turonian. Collapse of underlying caverns continues and sinkholes are widened by dissolution at the exposed surface; e) sea level rise and development of the foreland basin leads to deposition of the Coniacian-Maastrichtian sequence, and differential compaction generates depressions above the largest karst features; f) Paleocene-Eocene sedimentation infills the depressions on the Maastrichtian surface, developing onlap relationships between this surface and the deposited sediments.

5. Conclusions & Implications

- Seismic-scale karst features may be deep, wide and areally widespread, sub-seismic-scale karstic features (Figure 19) may be even more widespread.
- Weak relationship between sinkhole density and pre-existing tectonic features suggesting that faults acted as conduits to focus fluid flow at depth.
- Karstification can have both a positive and a negative effect on the porosity and permeability of a reservoir.
- Karst features and associated breccias may initially act as a conduit for fluid flow or enhance connectivity but increasing collapse of caverns, or the precipitation of cements from migrating fluids may also act to reduce poroperm
- On a field scale, workflows should integrate regional tectonostratigraphic analysis, regional to field-scale seismic analysis, and assessment of diagenetic processes through geochemical analysis and petrography.

Figure 19: Variable scales of sub-seismic porosity/karstification in the Sarvak Formation, Iran, ranging from large vugs (a) and caves (b) to intercrystalline porosity (c & d)

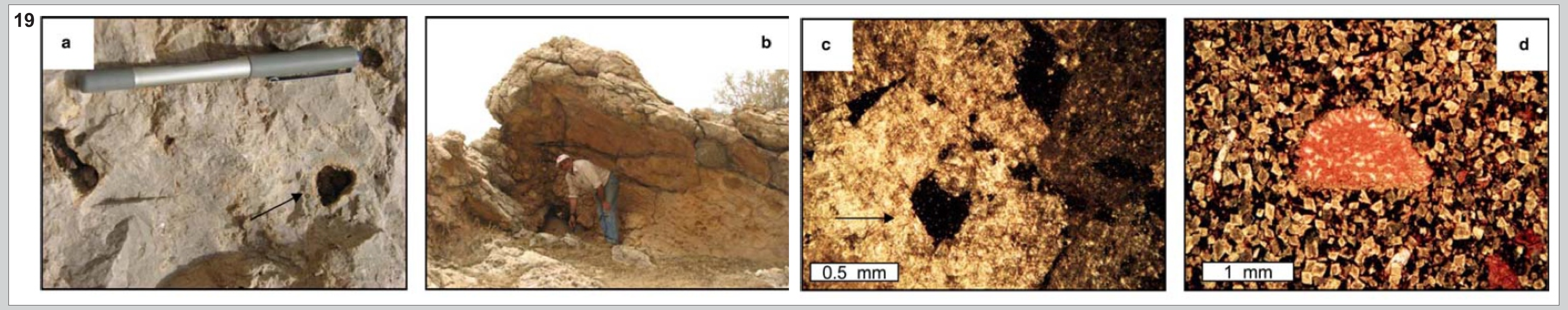

Acknowledgements: We thank GGS ASA for permission to use the PC-2000 dataset. We acknowledge IHS for an academic license for The Kingdom Suite. SRC acknowledges a UCARE grant from the University of Nebraska-Lincoln, funding her contribution to this project

References: **Alavi, M., 2004.** Regional stratigraphy of the Zagros fold-thrust belt of Iran and its proforeland evolution. American Journal of Science, 304 p1-20. **Hajikazemi, E., Al-Aasm, I.S. & Coniglio, M., 2010.** Subaerial exposure and meteoric diagenesis of the Cenomanian-Turonian Upper Sarvak Formation, southwestern Iran. In Leturmy, P. & Robin, C (eds). Tectonic and stratigraphic evolution of Zagros and Makran during the Mesozoic-Cenozoic. Geological Society of London Special Publication 330, p253-272. **Lucia, F.J., 1995.** Lower Paleozoic Cavern Development, Collapse, and Dolomitization, Franklin Mountains, El Paso, Texas. In Budd, D.A., saller, A.H. & Harris, P.M. (eds) Unconformities and Porosity in Carbonate strata. AAPG Memoir 63 p279-300 **Mehrabi, H. & Rahimpour-Bonab, H., 2014.** Paleoclimate and tectonic controls on the depositional and diagenetic history of the Cenomanian-early Turonian carbonate reservoirs, Dezful Embayment, SW Iran. Facies, 60, p147-167 **Swift, S. A., Uchupi, E. & Ross, D. A. 1998.** Late Cenozoic Geology of the central Persian (Arabian) Gulf from Industry Well data and Seismic profiles. WHOI Technical Memorandum 01-98, 76pp.